Focal Adhesion Kinase Targeting Using *In vivo* Short Interfering RNA Delivery in Neutral Liposomes for Ovarian Carcinoma Therapy

Jyotsnabaran Halder,[1] Aparna A. Kamat,[1] Charles N. Landen, Jr.,[1] Liz Y. Han,[1] Susan K. Lutgendorf,[5] Yvonne G. Lin,[1] William M. Merritt,[1] Nicholas B. Jennings,[1] Arturo Chavez-Reyes,[2] Robert L. Coleman,[1] David M. Gershenson,[1] Rosemarie Schmandt,[1] Steven W. Cole,[4] Gabriel Lopez-Berestein,[1] and Anil K. Sood[1,3]

Abstract

Purpose: Focal adhesion kinase (FAK) plays a critical role in ovarian cancer cell survival and in various steps in the metastatic cascade. Based on encouraging *in vitro* results with FAK silencing, we examined the *in vivo* therapeutic potential of this approach using short interfering RNA (siRNA) in the neutral liposome 1,2-dioleoyl-*sn*-glycero-3-phosphatidylcholine (DOPC).

Experimental Design: Therapy experiments of FAK siRNA with or without docetaxel were done using human ovarian cancer cell lines SKOV3ip1, HeyA8, and HeyA8MDR in nude mice. Additional experiments with a cisplatin-resistant cell line (A2780-CP20) were also done. Assessments of angiogenesis (CD31), cell proliferation (proliferating cell nuclear antigen), and apoptosis (terminal deoxynucleotidyl transferase–mediated dUTP nick end labeling) were done using immunohistochemical analysis.

Results: A single dose of FAK siRNA-DOPC was highly effective in reducing *in vivo* FAK expression for up to 4 days as assayed by Western blot and immunohistochemical analysis. Therapy experiments were started 1 week after injection of the ovarian cancer cells. Treatment with FAK siRNA-DOPC (150 μg/kg twice weekly) reduced mean tumor weight by 44% to 72% in the three cell lines compared with the control group (Ps < 0.05 for HeyA8, A2780-CP20, and SKOV3ip1). When FAK siRNA-DOPC was combined with docetaxel, there was even greater reduction in mean tumor weight in all models (all Ps < 0.05). Similar results were observed in combination with cisplatin. Treatment with FAK siRNA-DOPC plus docetaxel resulted in decreased microvessel density, decreased expression of vascular endothelial growth factor and matrix metalloproteinase-9, and increased apoptosis of tumor-associated endothelial cells and tumor cells.

Conclusions: Taken together, these findings suggest that FAK siRNA-DOPC plus docetaxel or platinum might be a novel therapeutic approach against ovarian cancer.

Ovarian cancer remains the leading cause of death from a gynecologic malignancy (1). Despite advances in surgical and chemotherapeutic approaches, most ovarian cancer patients develop recurrent disease and eventually succumb to their disease (2, 3). Given the high mortality rates of ovarian cancer,

development of novel therapeutic approaches is urgently needed.

Focal adhesion kinase (FAK) is a 125-kDa nonreceptor protein tyrosine kinase that plays a significant role in cell survival, migration, and invasion (4–10). Several studies have indicated that FAK has a direct role in tumor growth via signaling through the urokinase receptor, RAS, and extracellular signal-regulated kinase/mitogen-activated protein kinase (11, 12). We (13) and others (14) have found that FAK is overexpressed in ovarian cancer and is predictive of poor clinical outcome. Although the mechanisms underlying increased expression of FAK in tumor cells are not fully understood, FAK gene amplification has been noted in ovarian carcinoma (15). FAK has also been shown to be functionally important in ovarian cancer cell migration and invasion; the dominant-negative construct FAK-related nonkinase promoted FAK dephosphorylation and decreased the *in vitro* migration and invasion of these cells (13). FAK overexpression has also been reported to protect cells from stressors, including etoposide treatment in human leukemic cells by activating the phosphatidylinositol 3-kinase/Akt survival pathway with the concomitant activation of nuclear factor-κB and induction of inhibitor-of-apoptosis proteins (16). How FAK overexpression

is protective is not fully understood. We have shown recently that FAK is cleaved after treatment with docetaxel chemotherapy in a caspase-3-dependent manner and FAK silencing promoted docetaxel cytotoxicity in ovarian cancer cells (17). FAK is overexpressed by a large number of other human tumors as well, including colon, breast (18–20), thyroid (20), and head and neck (21) cancers. Thus, FAK is an attractive target for therapeutic intervention.

Short interfering RNA (siRNA) technology is an intriguing and powerful method of gene down-regulation, which has been widely used to study gene function and target discovery (22). However, *in vivo* siRNA delivery has been difficult to achieve with high efficiency. Although delivery of "naked" siRNA at specific local sites or with high-pressure means has been used in experimental models, these approaches are not clinically practical. Recently, we have shown highly efficient *in vivo* delivery of siRNA in an orthotopic model of ovarian carcinoma by using a neutral lipid liposome, 1,2-dioleoyl-*sn*-glycero-3-phosphatidylcholine (DOPC; ref. 23). Furthermore, in proof-of-principle studies with targeting the EphA2 receptor, this approach was therapeutically efficacious (23). Based on the known functions of FAK and promising *in vitro* results with FAK silencing, we investigated the *in vivo* antitumor effects of FAK silencing using siRNA incorporated in DOPC and revealed additional antiangiogenic effects on the tumor microenvironment.

Materials and Methods

Cell lines and cultures. The derivation and source of established human ovarian cancer cell lines SKOV3ip1, HeyA8, and A2780-CP20 have been described previously (23, 24). The taxane-resistant cell line HeyA8MDR (a gift from Dr. Isaiah Fidler, Department of Cancer Biology, University of Texas M. D. Anderson Cancer Center) was also used. As reported previously, the IC_{50} level for docetaxel for the HeyA8MDR cells is 450 nmol/L (17). These cell lines were selected because they were derived from women with advanced ovarian cancer and reflect the patterns of spread seen in human patients. All the cell lines were maintained and propagated *in vitro* by serial passage in RPMI 1640 or modified Eagle's medium supplemented with 15% fetal bovine serum and 0.1% gentamicin sulfate (Gemini Bioproducts, Calabasas, CA). All *in vitro* experiments were conducted with 70% to 80% confluent cultures.

siRNA synthesis. siRNAs were synthesized and then purified using high-performance liquid chromatography (Qiagen-Xeragon, Germantown, MD). FAK siRNA (target sequence 5′-AACCACCTGG-GCCAGTATTAT-3′) and control siRNA (target sequence 5′-AATTC-TCCGAACGTGTCACGT-3′) bearing no sequence homology with any known human mRNA sequences were dissolved in buffer [100 mmol/L potassium acetate, 30 mmol/L HEPES KOH, 2 mmol/L magnesium acetate (pH 7.4)] to a final concentration of 20 μmol/L, heated to 90°C for 60 seconds, incubated at 37°C for 60 minutes, and stored at −20°C until future use.

Liposomal siRNA preparation. siRNA for *in vivo* delivery was incorporated into the phospholipid DOPC. siRNA and DOPC were mixed in the presence of excess *t*-butanol at a ratio of 1:10 (w/w) as described previously (23). Tween 20 was added to the mixture, which was then vortexed, frozen in an acetone, dry ice bath, and lyophilized. Before *in vivo* administration, this preparation was hydrated with normal (0.9%) saline at a concentration of 15 μg/mL to achieve the desired dose in 150 to 200 μL/injection. The liposomal preparation is a preliposomal powder (lyophilizate) containing the lipid and the siRNA, thus providing long-term stability. Once reconstituted, the preparation should be used with 12 hours. Different batches of the preparation were used for the studies. All batches were lyophilized under the same conditions.

Western blot analysis. Cells were lysed in modified radioimmuno-precipitation assay buffer [50 mmol/L Tris, 150 mmol/L NaCl, 1% Triton, 0.5% deoxycholate + 25 μg/mL leupeptin, 10 μg/mL aprotinin, 2 mmol/L EDTA, 1 mmol/L sodium orthovanadate (Sigma, St. Louis, MO)] as described previously (13, 25). Lysates were clarified by centrifugation at 12,500 rpm for 30 minutes. The total protein concentration of the supernatant was determined using a bicinchoninic acid protein assay reagent kit (Pierce, Rockford, IL). Proteins were separated by 7.5% SDS-PAGE and transferred to nitrocellulose membrane by semidry transfer (Bio-Rad Laboratories, Hercules, CA). Membranes were blocked with 5% nonfat milk and incubated with 0.25 μg/mL anti-FAK antibody (Biosource International, Camarillo, CA) for 1 hour at room temperature. Antibody was detected with 0.167 μg/mL horseradish peroxidase (HRP)–conjugated anti-mouse secondary antibody (The Jackson Laboratory, Bar Harbor, ME) and developed with an enhanced chemiluminescence detection kit (Pierce). Equal loading was confirmed by detection of β-actin (0.1 μg/mL, anti-β-actin antibody; Sigma). Densitometric analysis was done using the Scion Imaging software (Scion Corp., Frederick, MD).

Reagents. Leupeptin, aprotinin, and sodium orthovanadate were obtained from Sigma, EDTA was from Life Technologies/Invitrogen (Carlsbad, CA), and docetaxel was from Sanofi-Aventis (Bridgewater, NJ). Primary antibodies used were mouse anti-FAK, mouse anti–proliferating cell nuclear antigen (PCNA) clone PC 10 (DAKO A/S, Copenhagen, Denmark), and mouse anti-CD31 (PharMingen, San Diego, CA). The following secondary antibodies were used for colorimetric immunohistochemical analysis: HRP-conjugated goat anti-rabbit IgG F(ab′)₂ (Jackson ImmunoResearch Laboratories, Inc., West Grove, PA), biotinylated mouse anti-goat (Biocare Medical, Walnut Creek, CA), HRP-conjugated streptavidin (DAKO), HRP-conjugated rat anti-mouse IgG2a (Serotec, Harlan Bioproducts for Science, Inc., Indianapolis, IN), HRP-conjugated goat anti-rat IgG (Jackson ImmunoResearch Laboratories), and fluorescent Alexa 488–conjugated goat anti-rabbit IgG (Molecular Probes, Inc., Eugene, OR).

Animal care and orthotopic implantation of tumor cells. Female athymic nude mice (NCr-*nu*) were purchased from the National Cancer Institute-Frederick Cancer Research and Development Center (Frederick, MD). The mice were housed and maintained under specific pathogen-free conditions in facilities approved by the American Association for Accreditation of Laboratory Animal Care and in accordance with current regulations and standards of the U.S. Department of Agriculture, U.S. Department of Health and Human Services, and NIH. All studies were approved and supervised by the University of Texas M. D. Anderson Cancer Center Institutional Animal Care and Use Committee. The mice were used in these experiments when they were 8 to 12 weeks old.

To produce tumors, SKOV3ip1, A2780-CP20, and HeyA8MDR (1×10^6 cells/0.2 mL HBSS) or HeyA8 (2.5×10^5 cells/0.2 mL HBSS) were injected i.p. into the mice. For *in vivo* injections, cells were trypsinized and centrifuged at 1,000 rpm for 7 minutes at 4°C, washed twice with PBS, and reconstituted in serum-free HBSS (Life Technologies/Invitrogen). Only single-cell suspensions with >95% viability, as determined by trypan blue exclusion, were used for the *in vivo* injections. Mice ($n = 10$ per group) were monitored for adverse effects of therapy and sacrificed on day 42 (SKOV3ip1) or day 28 (HeyA8, A2780-CP20, or HeyA8MDR) or when any of the mice began to appear moribund. Mouse weight, tumor weight, and tumor distribution were recorded. Tissue specimens were snap frozen for lysate preparation, fixed in formalin for paraffin embedding, or frozen on OCT compound (Miles, Inc., Elkhart, IN) for frozen slide preparation.

Therapy for established human ovarian carcinoma in the peritoneal cavity of nude mice. To evaluate the therapeutic effect of the combination of FAK siRNA and docetaxel in our mouse model, we first did preliminary dose-response experiments for FAK siRNA. HeyA8 cells were implanted i.p. and treatment was initiated 21 days following

tumor injection when i.p. tumors could be assessed by palpation. Mice were randomly distributed into three groups (*n* = 10 per group) and treated with a single dose of PBS, control siRNA-DOPC, or FAK siRNA-DOPC at 75, 150, or 300 μg/kg i.p. The i.p. route for siRNA delivery was selected based on comparable uptake and therapeutic efficacy with either i.p. or i.v. routes (26) in 200 μL volume. Following treatment, three mice were sacrificed at 24, 48, or 96 hours or 6 days. Immunohistochemical analysis was done on any excised peritoneal cavity tumors as described below. The 75 μg/kg dose yielded inconsistent FAK down-regulation. However, at both of the higher doses, consistent FAK down-regulation was observed (data not shown). Therefore, the 150 μg/kg dose was selected for all subsequent experiments. To determine the optimal dose of docetaxel, HeyA8-bearing nude mice were treated with either 20, 30, 40, 50, or 60 μg/wk i.p. docetaxel. The lowest effective dose in this model was 50 μg/wk (data not shown), which was selected for all subsequent experiments. Similarly, cisplatin doses ranging from 80 to 200 μg/wk i.p. were tested in the platinum-sensitive A2780-PAR model and the lowest effective dose of 160 μg (data not shown) was selected for subsequent experiments.

Based on the results of our preliminary dose-response experiments, we initiated a series of separate therapy experiments using the optimal FAK siRNA dosage. Tumor cells were injected i.p., and 7 days later, the mice (*n* = 10 per group) were randomly assigned to five treatment groups: empty liposome twice weekly, nonspecific control siRNA-DOPC (150 μg/kg) twice weekly, FAK siRNA-DOPC (150 μg/kg) twice weekly, control siRNA-DOPC in combination with 50 μg/wk docetaxel, and FAK siRNA-DOPC plus docetaxel. For the *in vivo* experiment with the cisplatin-resistant A2780-CP20 model, the therapy groups were the same, except 160 μg/wk i.p. cisplatin was used instead of docetaxel. At 7 days after tumor cell injection, small volume disease is present (24).

Toxicology analysis. Whole blood was obtained from animals (*n* = 3 per group) in all five therapy groups (described above) for standard complete blood count analysis before therapy on days 7 (baseline), 14, and 21.

Immunohistochemical determination of PCNA and CD31. Expression of PCNA was determined by immunohistochemical analysis using paraffin-embedded tumors. Sections (8-μm-thick) were deparaffinized in xylene, treated with a graded series of alcohol [100%, 95%, and 80% ethanol/double-distilled H_2O (v/v)], and rehydrated in PBS (pH 7.5). Antigen retrieval was done by microwave heating for 5 minutes in 0.1 mol/L citrate buffer (pH 6.0) followed by blocking of endogenous peroxide with 3% H_2O_2 in methanol for 5 minutes. After PBS washes, slides were blocked with 5% normal horse serum and 1% normal goat serum in PBS for 15 minutes at room temperature followed by incubation with primary antibody (anti-PCNA, PC-10, mouse IgG) in blocking solution overnight at 4°C. After two PBS washes, the appropriate secondary antibody conjugated to HRP, in blocking solution, was added for 1 hour at room temperature. HRP was detected with 3,3′-diaminobenzidine (Phoenix Biotechnologies, Huntsville, AL) substrate for 5 minutes, washed, and counterstained with Gill No. 3 hematoxylin (Sigma) for 20 seconds. Immunohistochemistry for CD31 was done on freshly cut frozen tissue. These slides were fixed in cold acetone for 10 minutes and did not require antigen retrieval. The primary antibody used was anti-CD31 (platelet/endothelial cell adhesion molecule-1, rat IgG; PharMingen). Staining for PCNA and CD31 was conducted on tumors collected at the conclusion of 4-week therapy trials. Control samples exposed to secondary antibody alone showed no specific staining.

Quantification of microvessel density, PCNA, and terminal deoxynucleotidyl transferase–mediated dUTP nick end labeling–positive cells. To quantify microvessel density (MVD), 10 random 0.159-mm² fields at ×100 final magnification were examined for each tumor (one slide per mouse, five slides per group) and the number of microvessels per field was counted by two investigators in a blinded fashion. A single microvessel was defined as a discrete cluster or single cell stained positive for CD31, and the presence of a lumen was required for scoring

as a microvessel. To quantify PCNA expression, the number of positive cells (3,3′-diaminobenzidine staining) was counted in 10 random 0.159-mm² fields at ×100 magnification. To quantify terminal deoxynucleotidyl transferase–mediated dUTP nick end labeling (TUNEL)–positive cells, the number of green fluorescence-positive cells was counted in 10 random 0.011-mm² fields at ×400 magnification.

Microscopic analysis. 3,3′-Diaminobenzidine-stained sections were examined with a ×10 objective on a Microphot-FX microscope (Nikon, Garden City, NY) equipped with a three-chip charge-coupled device color video camera (model DXC990, Sony, Tokyo, Japan). Immunofluorescence microscopy was done using a ×20 objective on a Microphot-FXA microscope (Nikon) equipped with a HBO 100 mercury lamp and narrow band-pass filters to individually select for green, red, and blue fluorescence (Chroma Technology, Brattleboro, VT). Images were captured using a cooled charge-coupled device camera (model 5810, Hamamatsu, Bridgewater, NJ) and Optimas Image Analysis software (Media Cybernetics, Silver Spring, MD). Photomontages were prepared using Micrografx Picture Publisher (Corel, Dallas, TX) and Adobe PhotoShop software (Adobe Systems, Inc., San Jose, CA). Photomontages were printed on a digital color printer (model UP-D7000, Sony).

Statistical analyses. For the *in vivo* experiments, differences in continuous variables (mean body weight, tumor weight, MVD, PCNA, and hematologic variables) were analyzed using the Student's *t* test for comparing two groups and by ANOVA for multiple group comparisons with $P < 0.05$ considered statistically significant. For values that were not normally distributed, the Mann-Whitney rank sum test was used. The Statistical Package for the Social Sciences (SPSS, Inc., Chicago, IL) was used for all statistical analyses.

Results

In vivo *down-regulation of FAK by siRNA.* Based on our prior data with regard to the effect of FAK-siRNA in sensitizing ovarian cancer cells to docetaxel (17), we investigated its *in vivo* therapeutic potential. Before initiating therapy experiments, we examined the ability of FAK-targeted siRNA incorporated in DOPC to down-regulate FAK *in vivo*. Nude mice bearing i.p. HeyA8 tumors were injected with a single dose of FAK siRNA-DOPC (150 μg/kg i.p.), and tumors were harvested 1, 2, 4, and 6 days after injection for Western blot analysis and immunohistochemistry for assessing level of FAK expression (17). Western blot analysis revealed >80% reduction in FAK levels within 48 hours, which persisted for at least 4 days (Fig. 1A). FAK expression began to return toward basal levels by 6 days after a single treatment. Similar results were noted with immunohistochemistry (Fig. 1B). FAK expression was not affected by control siRNA-DOPC. Therefore, we selected twice weekly administration of siRNA-DOPC as the optimal dosing schedule for subsequent therapy experiments.

In vivo *therapy experiments with FAK siRNA-DOPC.* The SKOV3ip1 or HeyA8 ovarian cancer cells were implanted into the peritoneal cavity of nude mice for experiments designed to test the therapeutic potential of FAK-targeted siRNA. Seven days later, therapy was started according to the five treatment groups listed above in Materials and Methods. The animals were sacrificed after 3 to 5 weeks of therapy and a necropsy was done. The data for the effects of these therapies on SKOV3ip1 and HeyA8 are summarized in Fig. 2A and B, respectively. Control siRNA therapy alone was not effective against SKOV3ip1 tumors compared with empty liposomes; however, ∼39% reduction was noted in the HeyA8 tumors (Fig. 2A and B). Treatment with FAK siRNA-DOPC alone or docetaxel plus control siRNA-DOPC was effective in inhibiting tumor growth
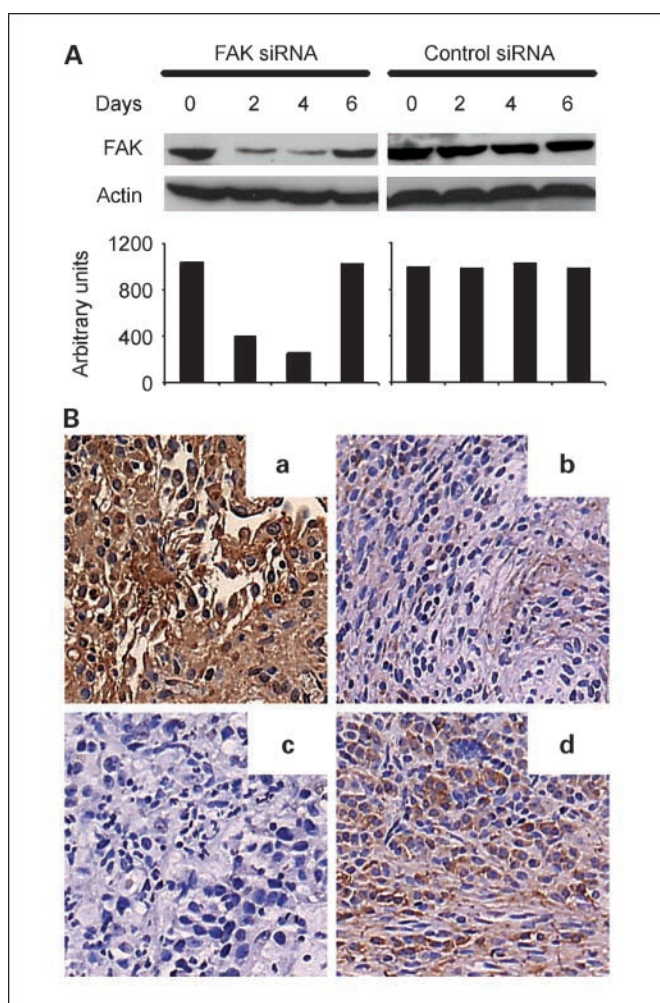
Fig. 1. *In vivo* down-regulation of FAK by FAK siRNA. *A,* Western blot of lysates from tumor samples collected 0, 2, 4, and 6 days after a single administration of FAK siRNA or control siRNA incorporated in DOPC. Quantification of band intensity relative to β-actin. *B,* immunohistochemical staining for FAK expression (original magnification, ×200) after treatment with control siRNA-DOPC (*a*) or FAK siRNA-DOPC 2 (*b*), 4 (*c*), and 6 (*d*) days after a single dose.

(54-74%) in both cell lines compared with control siRNA (Fig. 2). However, treatment with FAK siRNA-DOPC in combination with docetaxel resulted in even greater reduction in tumor weight (94-98%; overall ANOVA $P < 0.001$ for both cell lines). Furthermore, the combination therapy was statistically superior to docetaxel plus control siRNA-DOPC in each of the two trials ($P = 0.04$ for HeyA8 and 0.02 for SKOV3ip1).

Chemotherapy resistance is a common clinical problem in the management of ovarian carcinoma. Despite high response rates with initial therapy, most patients develop recurrent tumors that are resistant to taxane and platinum chemotherapy (2, 27, 28). We have shown previously that FAK down-regulation can sensitize even chemotherapy-resistant cell lines to docetaxel *in vitro* (17). This led us to examine whether FAK down-regulation could sensitize resistant tumors to chemotherapy using the HeyA8MDR cell line (Fig. 2C). Therapy was started 7 days after injection of tumor cells into nude mice according to the five groups outlined above. With this model, FAK siRNA-DOPC alone resulted in ∼44% reduction in tumor growth (Fig. 2C) compared with control. Furthermore, the

combination of FAK siRNA-DOPC and docetaxel was superior than docetaxel/control siRNA-DOPC ($P < 0.006$) and FAK siRNA-DOPC alone ($P < 0.05$). To evaluate the generality of these results, we also examined the efficacy of FAK siRNA-DOPC in combination with cisplatin in the platinum-resistant A2780-CP20 model. As expected, cisplatin monotherapy was not effective in this model (Fig. 3). Treatment with FAK siRNA-DOPC resulted in 72% decrease in the mean tumor weight compared with the control siRNA-DOPC group. The combination of FAK siRNA-DOPC with cisplatin was more effective than FAK siRNA-DOPC alone ($P < 0.02$), control siRNA-DOPC ($P < 0.001$), and control siRNA-DOPC/cisplatin ($P < 0.001$) groups.

Data from other measured variables of these therapy experiments are shown in Table 1. The incidence of tumor formation was not significantly reduced in either control siRNA-DOPC or control siRNA-DOPC plus docetaxel. FAK siRNA-DOPC treatment was associated with 70% tumor incidence in both of the cell lines individually, which was reduced to 50% and 60% by the combination treatment in the SKOV3ip1 and HeyA8 models, respectively. The number of tumor nodules was significantly lower in the FAK siRNA-DOPC and the combination groups across all models (Table 1). No obvious toxicities were observed in the animals during treatment as determined by behavioral changes, such as eating habits and mobility. Furthermore, mouse weights were not significantly different among the five groups of animals, suggesting that eating and drinking habits were not affected. We also did complete blood count analyses before therapy on days 7 (baseline), 14, and 21. There were no significant changes in WBC, hemoglobin, or platelet counts during therapy (Table 2).

At the conclusion of the therapy experiments, we examined whether FAK expression in HeyA8 cells remained suppressed. FAK levels were not suppressed in either control siRNA-DOPC, empty liposome, or control siRNA-DOPC plus docetaxel group (Fig. 4A). However, in the FAK siRNA-DOPC and combined FAK siRNA-DOPC with docetaxel groups, there was sustained suppression of FAK expression (Fig. 4A).

Effect of FAK targeting on angiogenesis, cell proliferation, and apoptosis. Although FAK suppression has been shown to have direct antitumor effects (17), emerging evidence suggests that there may also be effects on the tumor microenvironment. To determine potential mechanisms underlying the efficacy of anti-FAK-based therapy, we examined its effects on several biological end points, including angiogenesis (MVD), proliferation (PCNA), and apoptosis (TUNEL). Due to growing evidence related to FAK and tumor angiogenesis (29, 30), we first evaluated vessel density (Fig. 4B) in the tumors harvested from experiments described above. Compared with empty liposomes, the mean MVD was reduced in tumors treated with FAK siRNA-DOPC alone or control siRNA-DOPC with docetaxel (Ps = 0.008 and 0.009, respectively). The most significant reduction in MVD occurred in the combination therapy group (MVD 6 ± 2; $P < 0.001$). Based on recent studies suggesting suppression of vascular endothelial growth factor (VEGF) and matrix metalloproteinases (30–33), we examined tumors harvested from all groups for these proteins. Indeed, both VEGF and matrix metalloproteinase-9 expression (Fig. 4C and D) were substantially reduced in tumors from animals treated with FAK siRNA-DOPC alone or in combination with docetaxel, suggesting an antivascular mechanism. To further characterize the antivascular mechanism, we did dual-localization (CD31
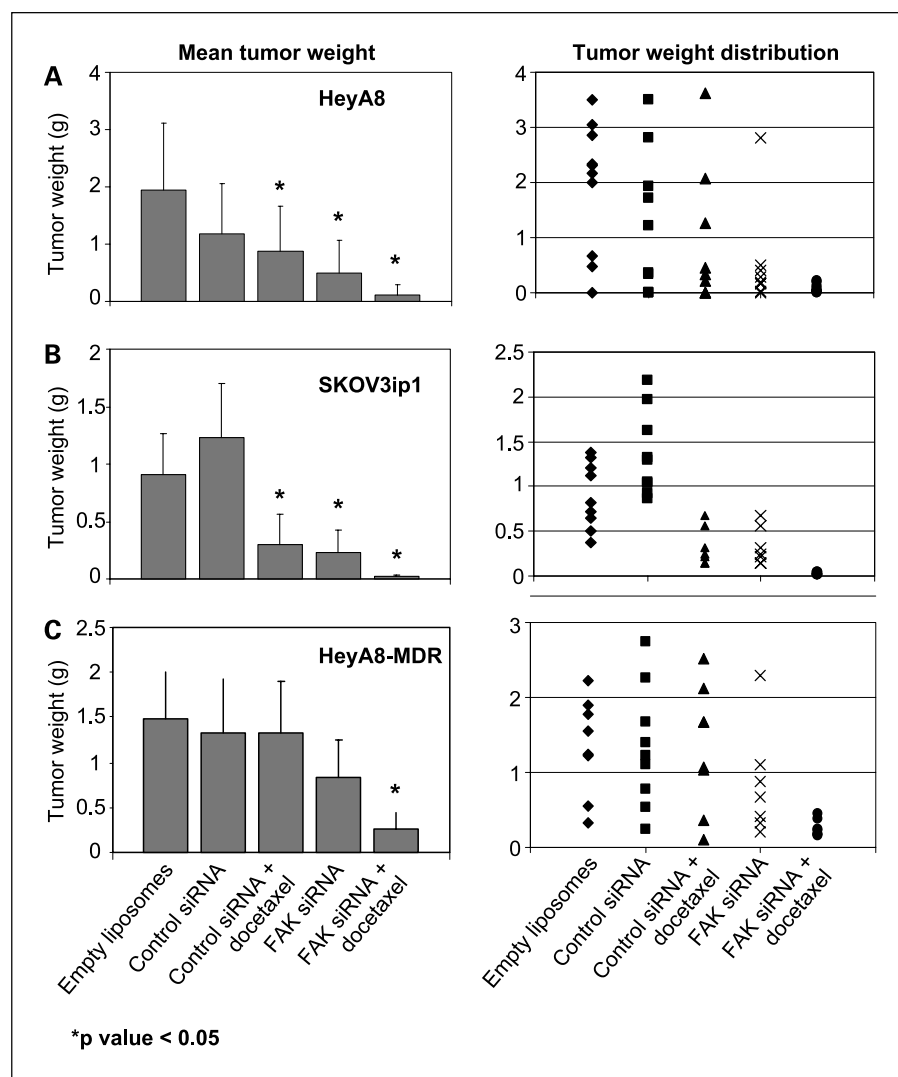
Fig. 2. Therapeutic efficacy of FAK siRNA with docetaxel. Nude mice were injected i.p. with HeyA8 (*A*), SKOV3ip1 (*B*), or HeyA8MDR (*C*) cells and randomly allocated to one of the following groups, with therapy beginning 1 week after tumor cell injection: empty DOPC liposomes, control siRNA in DOPC, control siRNA in DOPC + docetaxel, FAK siRNA in DOPC, and FAK siRNA in DOPC + docetaxel. The animals were sacrificed when control mice became moribund (3-5 weeks after starting therapy) and necropsy was done. Left, columns, mean tumor weights; bars, SD. Right, individual weights.

and TUNEL) immunofluorescence studies in tumors harvested after short-term treatment (3 days) in animals bearing formed HeyA8 tumors (17 days after tumor cell injection for all groups). Tumors treated with control siRNA had prominent vasculature with no apoptosis seen in endothelial cells (Fig. 4E). However, endothelial cell apoptosis was significantly increased in both FAK siRNA-DOPC and FAK siRNA-DOPC plus docetaxel-treated groups (both $Ps < 0.05$). To determine if
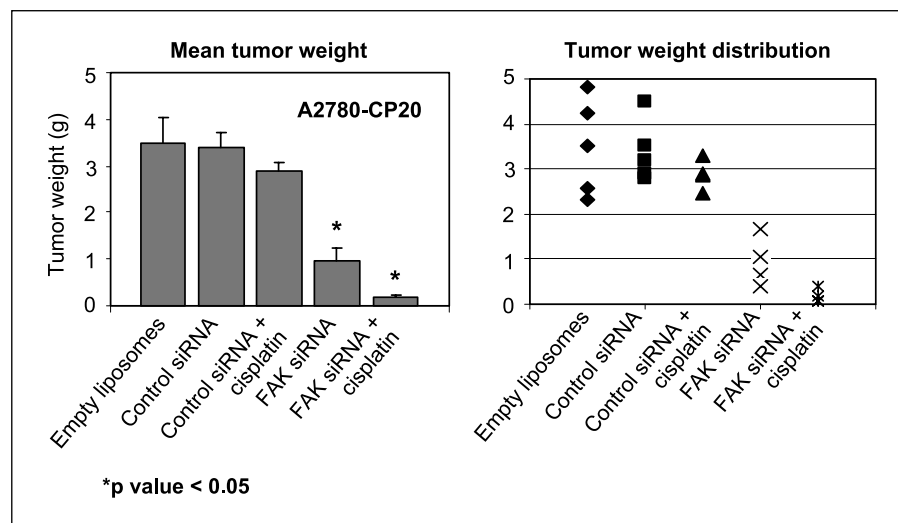
Fig. 3. Therapeutic efficacy of FAK siRNA with cisplatin. Nude mice bearing A2780-CP20 tumors were randomly allocated to one of the following groups, with therapy beginning 1 week after tumor cell injection: empty liposomes, control siRNA in DOPC, control siRNA in DOPC + cisplatin, FAK siRNA in DOPC, and FAK siRNA in DOPC + cisplatin. The animals were sacrificed when control mice became moribund (4 weeks after tumor cell injection) and necropsy was done. Left, columns, mean tumor weights; bars, SD. Right, individual weights.

Table 1. Characteristics of tumors after FAK siRNA-DOPC with or without chemotherapy

Cell line	Group	Incidence (%)	No. nodules (mean ± SE)	P for no. nodules
SKOV3ip1	Liposomes	100	16.6 ± 3.3	
	Control siRNA	100	15.4 ± 2.6	0.74
	Control siRNA + docetaxel	80	3.7 ± 1.1	0.008
	FAK siRNA	70	4.2 ± 0.7	<0.001
	FAK siRNA + docetaxel	50	1.6 ± 0.4	<0.001
HeyA8	Liposomes	100	4.4 ± 1.4	
	Control siRNA	100	4.0 ± 0.8	0.88
	Control siRNA + docetaxel	90	2.5 ± 0.9	0.009
	FAK siRNA	70	1.7 ± 0.4	0.004
	FAK siRNA + docetaxel	60	0.9 ± 0.3	<0.001
HeyA8MDR	Liposomes	90	4.3 ± 0.5	
	Control siRNA	90	4.4 ± 1.0	0.69
	Control siRNA + docetaxel	80	3 ± 1.2	0.48
	FAK siRNA	70	2.2 ± 0.4	0.002
	FAK siRNA + docetaxel	70	1.4 ± 0.4	<0.001
A2780-CP20	Liposomes	100	13.4 ± 1.3	
	Control siRNA	100	14.6 ± 1.9	0.51
	Control siRNA + cisplatin	80	11.5 ± 1.2	0.42
	FAK siRNA	80	5.0 ± 0.4	0.001
	FAK siRNA + docetaxel	100	1.8 ± 0.4	<0.001

FAK siRNA-DOPC-mediated *in vivo* effects on endothelial cells could be direct, we treated murine endothelial cells isolated from the ovary of ImmortoMice [H-2k(b)-tsA58; ref. 34] with FAK siRNA-DOPC. Murine FAK levels were not altered by the FAK siRNA-DOPC used for the *in vivo* experiments (data not shown).

Next, we examined the effects of FAK-targeted therapy on tumor cell proliferation by using PCNA staining. Minimal reduction of PCNA expression was observed by either control siRNA-DOPC plus docetaxel or FAK siRNA-DOPC compared with either empty liposome or control siRNA-DOPC treatment groups. PCNA expression was significantly reduced (21 ± 1.6%) in tumors from mice receiving FAK siRNA-DOPC with docetaxel (Fig. 4F). Finally, we evaluated tumor cell apoptosis

by using the TUNEL method. Minimal tumor cell apoptosis was apparent in either empty liposome, single agent, or control siRNA-DOPC with docetaxel treatment groups. Treatment with FAK siRNA-DOPC and docetaxel resulted in a significant increase in apoptosis (Fig. 4G).

Discussion

The key findings from the present study are that targeted therapy with FAK siRNA-DOPC in combination with chemotherapy significantly reduces tumor growth in both chemotherapy-sensitive and chemotherapy-resistant models. These effects are likely both direct and indirect (by inducing apoptosis in tumor-associated endothelial cells) at least in part due to reduction of

Table 2. Selected hematologic variables after siRNA with or without chemotherapy

Variables*	Day 7 (baseline)	Day 14	Day 21	P
Liposomes				
WBC	4.71 ± 0.16	3.99 ± 0.42	3.69 ± 0.76	0.63
Hemoglobin	16.50 ± 0.99	16.02 ± 1.27	14.30 ± 0.28	0.19
Platelets	708.5 ± 75.66	567.0 ± 41.01	752.0 ± 57.28	0.26
Control siRNA				
WBC	5.0 ± 0.13	4.12 ± 0.74	4.21 ± 0.54	0.38
Hemoglobin	14.85 ± 0.92	12.80 ± 2.55	14.80 ± 0.85	0.45
Platelets	622.0 ± 42.43	839.5 ± 67.2	755.0 ± 138.6	0.50
Control siRNA + cisplatin				
WBC	4.77 ± 0.07	3.78 ± 0.8	4.04 ± 0.33	0.60
Hemoglobin	12.50 ± 0.99	13.05 ± 1.77	13.30 ± 2.55	0.91
Platelets	605.0 ± 66.5	799.0 ± 87.7	664.0 ± 172.5	0.36
FAK siRNA				
WBC	4.97 ± 0.03	3.2 ± 0.11	5.67 ± 0.49	0.007
Hemoglobin	13.65 ± 0.64	16.04 ± 0.48	14.45 ± 0.92	0.09
Platelets	602.0 ± 84.8	751.5 ± 156.3	590.0 ± 41.1	0.36
FAK siRNA + cisplatin				
WBC	4.91 ± 0.13	4.58 ± 0.35	4.60 ± 1.8	0.94
Hemoglobin	13.45 ± 0.92	14.85 ± 0.35	13.70 ± 0.42	0.20
Platelets	663.0 ± 166.9	702.0 ± 57.9	553.5 ± 136.4	0.56

NOTE: Values expressed as mean ± SD.
*WBC expressed as 10^3 cells/μL; hemoglobin expressed as g/dL, and platelets expressed as 10^3 cells/μL.
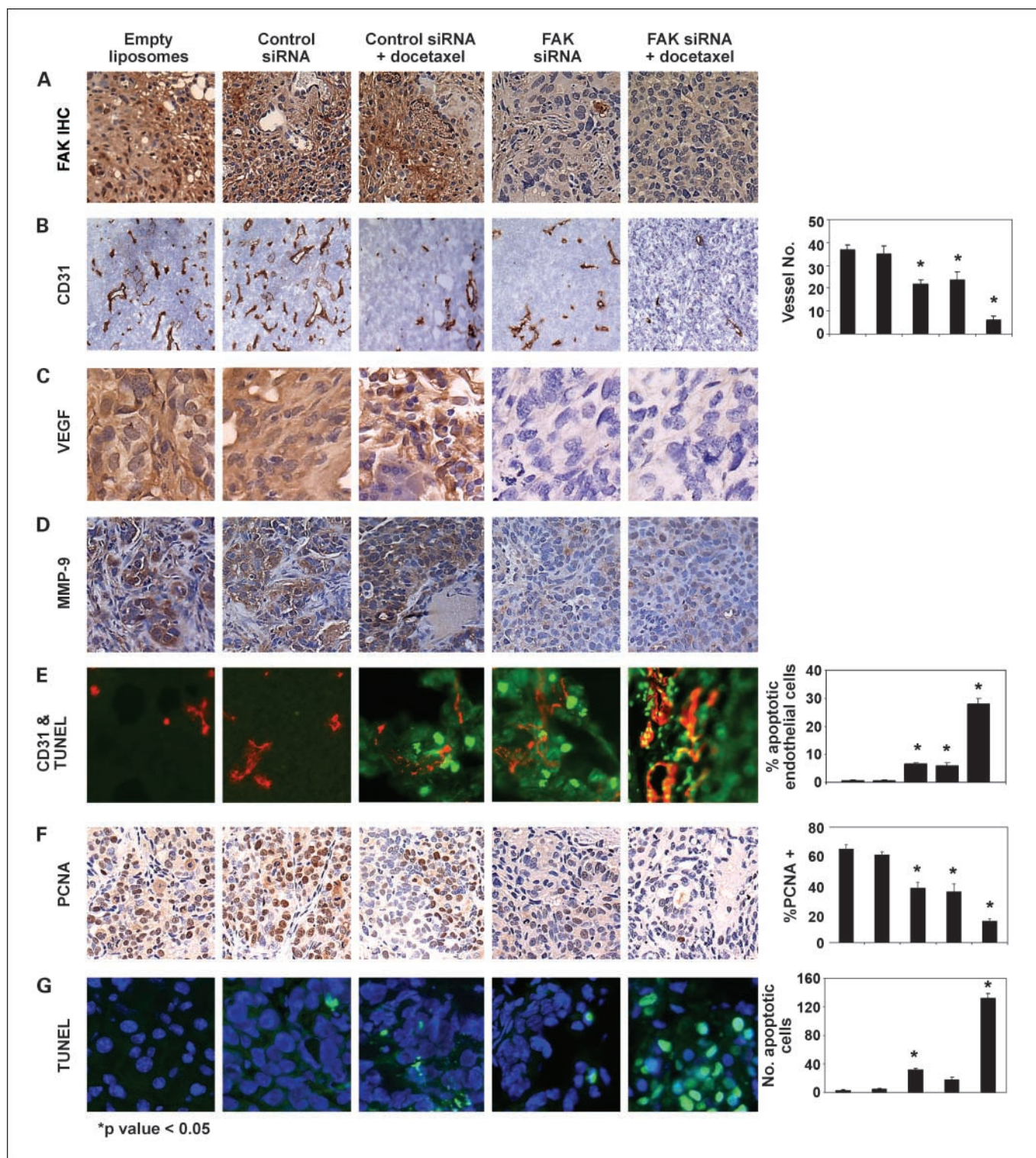
Fig. 4. *A,* immunohistochemistry (*IHC*) of FAK expression after long-term therapy in the HeyA8 orthotopic model. *B,* MVD was determined after immunohistochemical peroxidase staining for CD31. The number of vessels per ×100 field were counted as described in Materials and Methods. Representative slides from each group and average number of vessels per field. Five fields per slide and at least three slides per group were examined. VEGF (*C*) and matrix metalloproteinase-9 (*MMP-9*; *D*) immunohistochemical peroxidase staining was done on tumor sections obtained from each of the five therapy groups. *E,* representative images of immunofluorescence staining with CD31⁺ cells (*red*) and cells undergoing apoptosis (TUNEL stain; *green*). Yellow, endothelial cells (*red*) undergoing apoptosis (*green*). *F,* tumor sections from each group were stained for PCNA. The number of cancer cell nuclei that were strongly PCNA positive were counted and divided by the total number of cells. Representative sections from each group. Original magnification, ×100. Columns, mean percentage of PCNA-positive cells; bars, SD. Four fields per slide and at least three slides per group (all from different animals) were counted. *G,* immunofluorescence staining with TUNEL (*green*) for apoptosis and Hoechst (*blue*) for nuclei was done. Representative slides from each group. The number of apoptotic cells (*green*) was counted. Columns, mean number of TUNEL-positive cells; bars, SD. Four fields per slide and at least three slides per group (all from different animals) were counted. The columns in all graphs correspond to the labeled columns in the picture.

VEGF. Given the clinical relationship between FAK and ovarian cancer prognosis (13), these findings implicate FAK as an attractive therapeutic target in ovarian cancer.

FAK is a nonreceptor kinase that is a critical mediator of signaling events between cells and their extracellular matrix (35, 36). It is tyrosine phosphorylated upon integrin binding or ligand binding by growth factor receptors (37, 38). FAK activation at focal adhesion sites leads to cytoskeletal reorganization, cellular adhesion, and survival, and it is known to play a role in cell migration and invasion (13). Several reports have linked FAK expression with cancer progression. FAK overexpression has been reported in many malignancies, including ovarian, colon, breast, and head and neck cancers (17–21). Specifically, in ovarian cancer, FAK is overexpressed in ~68% of tumors and is associated with high-risk clinical features and poor survival (13). Although the mechanisms behind FAK overexpression are not fully known, we have recently found that FAK gene amplification is present in ovarian cancers (15). We have also shown previously that FAK is a substrate for caspase-3 and is degraded during treatment with docetaxel in sensitive cells (17). Prior *in vitro* studies prompted us to examine the therapeutic efficacy of FAK silencing *in vivo*, and to the best of our knowledge, our study is the first to use a clinically relevant delivery system for FAK siRNA in an orthotopic model of ovarian cancer. In the current study, therapy was started with low-volume ovarian carcinoma. Although we have shown siRNA delivery into larger tumors previously (23), whether FAK inhibition has therapeutic efficacy with bulkier tumors remains to be determined.

Although FAK silencing seems to have direct antitumor activity, there is growing evidence that the tumor microenvironment may also be affected. Sheta et al. showed that cell contact-mediated induction of VEGF transcription occurs via FAK (39). In an elegant study, Mitra et al. showed that 4T1 breast cancer tumors with inhibited FAK activity were substantially smaller compared with controls and exhibited less VEGF staining (30). Furthermore, cells with mutant FAK had impaired VEGF production and reduced tumor growth *in vivo* (30). In our experiments, FAK silencing was associated with lower levels of VEGF and matrix metalloproteinase-9 and increased apoptosis of tumor-associated endothelial cells, suggesting an antivascular effect.

Because of the pivotal role of FAK in many processes associated with cancer progression, interfering with its function may represent novel therapeutic opportunities. Investigators are developing various strategies for targeting FAK. Strategies aimed at inhibiting FAK kinase activity are being devised (40). Small-molecule inhibitors that act as competitors for ATP binding at the catalytic site are also being developed. We and others are using siRNA for down-regulating FAK using approaches that may hold promise for clinical use. We have shown previously the feasibility of delivering gene-specific siRNA using DOPC liposomes in orthotopic ovarian cancer models (23). This approach is more efficient for *in vivo* siRNA delivery than either naked siRNA or cationic liposomes. In the current study, we used specific FAK siRNA in DOPC liposomes for systemic delivery, which resulted in efficient FAK down-regulation and therapeutic efficacy. The importance of this work is that the packaging of siRNA into liposomes is rapidly transferable to a clinical setting for cancer therapeutics. It is possible that this delivery method may also be useful for noncancerous diseases

amenable to siRNA therapy (41–43). This technique is not tissue specific, but further modifications of the liposome may allow tumor-selective delivery (44, 45).

Several other approaches for delivering siRNA *in vivo* have been attempted. Duxbury et al. showed that systemic delivery of naked siRNA targeting FAK (46) or EphA2 (47) down-regulated protein expression and slowed the growth of a single s.c. injected malignant pancreatic cell line. Sorensen et al. showed the reduction of tumor necrosis factor-α expression in liver and spleen by delivering siRNA packaged in cationic liposomes (48). Others have used rapid injection of a high volume of material (i.e., 2 mL into a mouse with an estimated 4 mL total blood volume) hydrodynamically forcing siRNA into the liver (42). However, such techniques are likely not practical in a clinical setting.

We investigated FAK silencing using a neutral liposome delivery method for several reasons. Liposomes are already being clinically used for chemotherapy and other delivery systems. Liposomes are a form of nanoparticles that function as carriers and act as a slow-release depot for the drug in the diseased tissue. Optimal liposome size depends on the tumor target. In tumor tissue, the vasculature is discontinuous, and pore sizes vary from 100 to 780 nm (49). By comparison, pore size in normal vascular endothelium is <2 nm in most tissues and 6 nm in postcapillary venules. Most liposomes are 65 to 125 nm in diameter. Negatively charged liposomes were believed to be more rapidly removed from circulation than neutral or positively charged liposomes; however, recent studies have indicated that the type of negatively charged lipid affects the rate of liposome uptake by the reticuloendothelial system. For example, liposomes containing negatively charged lipids that are not sterically shielded (phosphatidylserine, phosphatidic acid, and phosphatidylglycerol) are cleared more rapidly than neutral liposomes. Cationic liposomes are not ideal delivery vehicles for tumor cells because surface interactions with the tumor cells create an electrostatically derived binding site barrier effect, inhibiting further association of the delivery systems with tumor spheroids (50). By comparison, neutral liposomes seem to have better intratumoral penetration.

Toxicity with specific liposomal preparations has also been a concern. Cationic liposomes elicit dose-dependent toxicity and pulmonary inflammation by promoting release of reactive oxygen intermediates, and this effect is more pronounced with multivalent cationic liposomes than monovalent cationic liposomes, such as *N*-[1-(2,3-dioleoyloxyl)propyl]-*N,N,N*-trimethylammonium methyl sulfate (51). Neutral and negative liposomes do not seem to exhibit lung toxicity (52). Cationic liposomes, while efficiently taking up nucleic acids, have had limited success for *in vivo* gene down-regulation perhaps because of their stable intracellular nature and resultant failure to release siRNA contents. We selected DOPC because of its neutral properties and prior success in using this vehicle to deliver antisense oligonucleotides *in vivo* without toxicity.

In summary, we have shown that FAK siRNA using a neutral liposomal system is highly effective for down-regulating FAK expression *in vivo*. Furthermore, treatment with FAK siRNA-DOPC plus chemotherapy was highly effective in inhibiting ovarian cancer growth by both direct and indirect antivascular mechanisms. These findings suggest that FAK siRNA in combination with either docetaxel or cisplatin chemotherapy could be a potent therapeutic combination against ovarian cancer even in patients with chemotherapy-resistant tumors.

References

1. Jemal A, Murray T, Ward E, et al. Cancer statistics, 2005. CA Cancer J Clin 2005;55:10–30.

2. McGuire WP, Hoskins WJ, Brady MF, et al. Cyclophosphamide and cisplatin compared with paclitaxel and cisplatin in patients with stage III and stage IV ovarian cancer.[comment]. N Engl J Med 1996; 334:1–6.

3. du Bois A, Luck HJ, Bauknecht T, et al. First-line chemotherapy with epirubicin, paclitaxel, and carboplatin for advanced ovarian cancer: a phase I/II study of the Arbeitsgemeinschaft Gynakologische Onkologie Ovarian Cancer Study Group. J Clin Oncol 1999;17:46–51.

4. Kohno M, Hasegawa H, Miyake M, et al. CD151 enhances cell motility and metastasis of cancer cells in the presence of focal adhesion kinase. Int J Cancer 2002;97:336–43.

5. Schaller MD, Parsons JT. Focal adhesion kinase: an integrin-linked protein tyrosine kinase. Trends Cell Biol 1993;3:258–62.

6. Schaller MD, Hildebrand JD, Parsons JT. Complex formation with focal adhesion kinase: a mechanism to regulate activity and subcellular localization of Src kinases. Mol Biol Cell 1999;10:3489–505.

7. Schaller MD. The focal adhesion kinase. J Endocrinol 1996;150:1–7.

8. Schaller MD. Focal adhesion kinase: an integrin-linked protein tyrosine kinase. Trends Cell Biol 1993;3: 258–62.

9. Hsia DA, Mitra SK, Hauck CR, et al. Differential regulation of cell motility and invasion by FAK. J Cell Biol 2003;160:753–67.

10. Sieg DJ, Hauck CR, Ilic D, et al. FAK integrates growth-factor and integrin signals to promote cell migration. Nat Cell Biol 2000;2:249–56.

11. Aguirre Ghiso JA. Inhibition of FAK signaling activated by urokinase receptor induces dormancy in human carcinoma cells *in vivo*. Oncogene 2002;21: 2513–24.

12. Hecker TP, Grammer JR, Gillespie GY, et al. Focal adhesion kinase enhances signaling through the Shc/extracellular signal-regulated kinase pathway in anaplastic astrocytoma tumor biopsy samples. Cancer Res 2002;62:2699–707.

13. Sood AK, Coffin JE, Schneider GB, et al. Biological significance of focal adhesion kinase in ovarian cancer: role in migration and invasion. Am J Pathol 2004; 165:1087–95.

14. Judson PL, He X, Cance WG, et al. Overexpression of focal adhesion kinase, a protein tyrosine kinase, in ovarian carcinoma. Cancer 1999;86:1551–6.

15. Bonome T, Lee JY, Park DC, et al. Expression profiling of serous low malignant potential, low-grade, and high-grade tumors of the ovary. Cancer Res 2005;65: 10602–12.

16. Sonoda Y, Matsumoto Y, Funakoshi M, et al. Anti-apoptotic role of focal adhesion kinase (FAK). Induction of inhibitor-of-apoptosis proteins and apoptosis suppression by the overexpression of FAK in a human leukemic cell line, HL-60. J Biol Chem 2000;275: 16309–15.

17. Halder J, Landen CN, Jr., Lutgendorf SK, et al. Focal adhesion kinase silencing augments docetaxel-mediated apoptosis in ovarian cancer cells. Clin Cancer Res 2005;11:8829–36.

18. Cance WG, Harris JE, Iacocca MV, et al. Immunohistochemical analyses of focal adhesion kinase expression in benign and malignant human breast and colon tissues: correlation with preinvasive and invasive phenotypes. Clin Cancer Res 2000;6:2417–23.

19. Han NM, Fleming RY, Curley SA, et al. Overexpression of focal adhesion kinase (p125FAK) in human colorectal carcinoma liver metastases: independence from c-src or c-yes activation. Ann Surg Oncol 1997; 4:264–8.

20. Owens LV, Xu L, Craven RJ, et al. Overexpression of the focal adhesion kinase (p125FAK) in invasive human tumors. Cancer Res 1995;55:2752–5.

21. Kornberg LJ. Focal adhesion kinase expression in oral cancers. Head Neck 1998;20:634–9.

22. Hannon GJ, Rossi JJ. Unlocking the potential of the human genome with RNA interference. Nature 2004; 431:371–8.

23. Landen CN, Jr., Chavez-Reyes A, Bucana C, et al. Therapeutic EphA2 gene targeting *in vivo* using neutral liposomal small interfering RNA delivery. Cancer Res 2005;65:6910–8.

24. Thaker PH, Yazici S, Nilsson MB, et al. Antivascular therapy for orthotopic human ovarian carcinoma through blockade of the vascular endothelial growth factor and epidermal growth factor receptors. Clin Cancer Res 2005;11:4923–33.

25. Sood AK, Seftor EA, Fletcher MS, et al. Molecular determinants of ovarian cancer plasticity. Am J Pathol 2001;158:1279–88.

26. Landen CN, Chavez-Reyes A, Bucana C, et al. Intraperitoneal delivery of liposomal siRNA for therapy of advanced ovarian cancer. Proc Am Assoc Cancer Res 2006;47:5462.

27. Vasey PA. Role of docetaxel in the treatment of newly diagnosed advanced ovarian cancer. J Clin Oncol 2003;21:136–44.

28. Fracasso PM, Brady MF, Moore DH, et al. Phase II study of paclitaxel and valspodar (PSC 833) in refractory ovarian carcinoma: a gynecologic oncology group study. J Clin Oncol 2001;19:2975–82.

29. Kornberg LJ, Shaw LC, Spoerri PE, et al. Focal adhesion kinase overexpression induces enhanced pathological retinal angiogenesis. Invest Ophthalmol Vis Sci 2004;45:4463–9.

30. Mitra S, Molina J, Hanson D, et al. Focal adhesion kinase (FAK) activity promotes tumor growth and neo-vascularization via upregulation of angiogenic factors. Proc Am Assoc Cancer Res 2005;46:475 [abstr 2029].

31. Mitra SK, Hanson DA, Schlaepfer DD. Focal adhesion kinase: in command and control of cell motility. Nat Rev Mol Cell Biol 2005;6:56–68.

32. Shibata K, Kikkawa F, Nawa A, et al. Both focal adhesion kinase and c-Ras are required for the enhanced matrix metalloproteinase 9 secretion by fibronectin in ovarian cancer cells. Cancer Res 1998;58:900–3.

33. Sein TT, Thant AA, Hiraiwa Y, et al. A role for FAK in the concanavalin A-dependent secretion of matrix metalloproteinase-2 and -9. Oncogene 2000;19: 5539–42.

34. Langley RR, Ramirez KM, Tsan RZ, et al. Tissue-specific microvascular endothelial cell lines from H-2K(b)-tsA58 mice for studies of angiogenesis and metastasis. Cancer Res 2003;63:2971–6.

35. Schaller MD. Biochemical signals and biological responses elicited by the focal adhesion kinase. Biochim Biophys Acta 2001;1540:1–21.

36. Schlaepfer DD, Hauck CR, Sieg DJ. Signaling through focal adhesion kinase. Prog Biophys Mol Biol 1999;71:435–78.

37. Schlaepfer DD, Hunter T. Integrin signalling and tyrosine phosphorylation: just the FAKs? Trends Cell Biol 1998;8:151–7.

38. Casamassima A, Rozengurt E. Insulin-like growth factor I stimulates tyrosine phosphorylation of p130(Cas), focal adhesion kinase, and paxillin. Role of phosphatidylinositol 3′-kinase and formation of a p130(Cas). Crk complex. J Biol Chem 1998;273: 26149–56.

39. Sheta EA, Harding MA, Conaway MR, et al. Focal adhesion kinase, Rap1, and transcriptional induction of vascular endothelial growth factor. J Natl Cancer Inst 2000;92:1065–73.

40. McLean GW, Avizienyte E, Frame MC. Focal adhesion kinase as a potential target in oncology. Expert Opin Pharmacother 2003;4:227–34.

41. Devroe E, Silver PA. Therapeutic potential of retroviral RNAi vectors. Expert Opin Biol Ther 2004;4:319–27.

42. McCaffrey AP, Meuse L, Pham TT, et al. RNA interference in adult mice. Nature 2002;418:38–9.

43. Lori F, Guallini P, Galluzzi L, et al. Gene therapy approaches to HIV infection. Am J Pharmacogenomics 2002;2:245–52.

44. Park JW, Hong K, Kirpotin DB, et al. Anti-HER2 immunoliposomes for targeted therapy of human tumors. Cancer Lett 1997;118:153–60.

45. Dubey PK, Mishra V, Jain S, et al. Liposomes modified with cyclic RGD peptide for tumor targeting. J Drug Target 2004;12:257–64.

46. Duxbury MS, Ito H, Benoit E, et al. RNA interference targeting focal adhesion kinase enhances pancreatic adenocarcinoma gemcitabine chemosensitivity. Biochem Biophys Res Commun 2003;311: 786–92.

47. Duxbury MS, Ito H, Zinner MJ, et al. CEACAM6 gene silencing impairs anoikis resistance and *in vivo* metastatic ability of pancreatic adenocarcinoma cells. Oncogene 2004;23:465–73.

48. Sorensen DR, Leirdal M, Sioud M. Gene silencing by systemic delivery of synthetic siRNAs in adult mice. J Mol Biol 2003;327:761–6.

49. Siwak DR, Tari AM, Lopez-Berestein G. The potential of drug-carrying immunoliposomes as anticancer agents. Commentary re: J.W. Park et al., Anti-HER2 immunoliposomes: enhanced efficacy due to targeted delivery. Clin Cancer Res 2002;8:955–6.

50. Kostarelos K, Emfietzoglou D, Papakostas A, et al. Binding and interstitial penetration of liposomes within avascular tumor spheroids. Int J Cancer 2004;112: 713–21.

51. Dokka S, Toledo D, Shi X, Castranova V, Rojanasakul Y. Oxygen radical-mediated pulmonary toxicity induced by some cationic liposomes. Pharm Res 2000; 17:521–5.

52. Gutierrez-Puente Y, Tari AM, Stephens C, Rosenblum M, Guerra RT, Lopez-Berestein G. Safety, pharmacokinetics, and tissue distribution of liposomal P-ethoxy antisense oligonucleotides targeted to Bcl-2. J Pharmacol Exp Ther 1999;291:865–9.